Ab Initio MO Study of the Unimolecular Decomposition of the Phenyl Radical

L. K. Madden, L. V. Moskaleva, S. Kristyan, and M. C. Lin*

Department of Chemistry, Emory University, Atlanta, Georgia 30322

Received: February 26, 1997; In Final Form: May 13, 1997[⊗]

The unimolecular decomposition of the C_6H_5 radical has been studied by ab initio molecular orbital and statistical-theory calculations. Three low-energy decomposition channels, including the commonly assumed decyclization/fragmentation process yielding *n*-$C_4H_3 + C_2H_2$, have been identified. With a modified Gaussian-2 method of Mebel et al. (ref 17), the energy barrier for the decyclization of C_6H_5 was calculated to be 66.5 kcal/mol with the corresponding recyclization energy of 5.6 kcal/mol. The two open-chain 1-dehydrohexa-1,3-dien-5-yne radicals (with HCĊH cis and trans structures) may undergo further fragmentation reactions producing *n*-$C_4H_3 + C_2H_2$ and *l*-C_6H_4 (1,5-hexadiyn-3-ene) + H with the predicted barriers of 44.0 and 36.1 kcal/mol, respectively. The dominant decomposition channel of C_6H_5 was found to take place barrierlessly by C−H breaking, producing *o*-C_6H_4 (*o*-benzyne) + H with the predicted endothermicity of 76.0 kcal/mol. RRKM calculations have been carried out for the production of *n*-$C_4H_3 + C_2H_2$, *l*-C_6H_4 + H, and *o*-C_6H_4 + H with the coupled multichannel mechanism, which includes the reversible decyclization/recyclization reactions. The results of the calculations indicate that at $T < 1500$ K *o*-C_6H_4 is the major product of the decomposition reaction. Above 1500 K, the formation of *l*-C_6H_4 becomes competitive with its cyclic isomer. However, the formation of the commonly assumed *n*-$C_4H_3 + C_2H_2$ products was found to be least competitive. Rate constants for all three product channels from C_6H_5 as well as those from the bimolecular reaction of *n*-C_4H_3 with C_2H_2 producing C_6H_5, *o*-C_6H_4 + H, and *l*-C_6H_4 + H have been calculated as functions of temperature and pressure for practical applications.

I. Introduction

The phenyl radical plays a pivotal role in the combustion of small aromatic hydrocarbons (key additives to lead-free gasoline) and the formation of polycyclic aromatic hydrocarbons (PAHs, precursors to soot).[1−5] Accordingly, there has been considerable interest in its reactions with combustion species[5−10] as well as its decomposition kinetics and mechanism at high temperatures.[11−14] In the present study, we focus on the latter aspects of the phenyl reaction by thoroughly exploring the energetics of all possible low-energy decomposition steps and the global rate constant for the decomposition reaction involving those individual channels.

To date, most theoretical calculations and kinetic simulations of reaction systems involving the phenyl radical (hereafter denoted by *c*-C_6H_5) assume invariably that its decomposition reaction occurs by decyclization, producing a linear open-chain radical, CH≡C−CH═CH−CH═ĊH (1-dehydrohexa-1,3-dien-5-yne), or *l*-C_6H_5, followed by the assumed rapid fragmentation reaction producing *n*-$C_4H_3 + C_2H_2$, viz.,[11−16]

$$c\text{-}C_6H_5 \xrightarrow{a} l\text{-}C_6H_5$$

$$l\text{-}C_6H_5 \xrightarrow{b} n\text{-}C_4H_3 + C_2H_2$$

The above assumption failed to consider the fact that the barrier for the fragmentation of *l*-C_6H_5, E°_b, is substantially higher than that for the recyclization, E°_{-a}, and that the overall energy for the production of *n*-$C_4H_3 + C_2H_2$ from *c*-C_6H_5 is considerably greater than that required for the formation of *o*-C_6H_4 (ortho benzyne) + H:

$$c\text{-}C_6H_5 \xrightarrow{c} o\text{-}C_6H_4 + H$$

The enthalpy changes associated with the formation of various products from *c*-C_6H_5 at 0 K can be found in Table 1 (vide infra).

In the present investigation, we employ a modified Gaussian-2 method, which has been developed by Mebel et al.[17] for accurate calculations of the ground electronic state energies of species containing up to seven heavy atoms.[18] The computation method was applied to examine the potential energy surface (PES) of the C_6H_5 ground electronic system, including the above three decomposition channels and the production of H + *l*-C_6H_4 (1,5-hexadiyn-3-ene) from the *c*-C_6H_5 radical. The results of this study are relevant to both thermally induced[11−14] and photo-initiated[19] fragmentation of *c*-C_6H_5.

II. Computation Methods

The G2M method of Mebel et al.,[17] employed in the present calculation, is a derivative of the original Gaussian-2 (G2) method of Pople and co-workers.[20] The latter uses a series of MP2, MP4 (Møller−Plessett second-/fourth-order perturbation), and QCISD(T) [quadratic configuration interactions with single, double (triple) substitutions] calculations employing various basis sets to approximate QCISD(T)/6-311+G(3df,2p)//MP2/6-31G(d) calculations with an additional "higher level correction" based on the number of paired and unpaired electrons.[20] Although the G2 method performs well for systems containing two or three heavy atoms, it has limitations associated with spin contamination and the use of scaled HF/6-31G(d) frequencies for zero-point-energy (ZPE) corrections as pointed out by Mebel et al.[17]

Different schemes of the G2M method have been developed to treat chemical systems of varying sizes.[17] For the present

* Corresponding author. E-mail address: chemmcl@emory.edu.
⊗ Abstract published in *Advance ACS Abstracts,* July 15, 1997.

S1089-5639(97)00723-8 CCC: $14.00

TABLE 1: Relative Energies (Zero-Point-Energy-Corrected, in kcal/mol) for Species Involved in Phenyl Radical Decomposition

species	ZPE[a]	B3LYP/6-31G(d)	UMP2/6-311+G(3df,2p)	PUMP4/6-311G(d,p)	RCCSD(T)/6-31G(d)	G2M (rcc,MP2)
phenyl radical[b] (C_{2v}, $^2A_1$)	54.9	0.0	0.0	0.0	0.0	0.0
benzyne (C_{2v}, $^1A_1$) + H	47.3	87.3	51.1	69.5	74.1	76.0
TS1 (C_s, $^2A'$)	50.2	71.7	84.2	65.6	69.4	66.5
INT1 (C_s, $^2A'$)	50.8	67.1	70.3	59.5	64.6	60.9
TS2 (C_s, $^2A'$)	49.7	71.1	74.4	62.6	69.0	64.9
INT2 (C_s, $^2A'$)	51.1	67.6	71.1	59.5	64.6	61.6
TS3 (C_1)	47.0	114.8	112.4	99.8	110.9	105.6
n-C_4H_3 (C_1) + C_2H_2	46.3	111.7	99.8	93.9	103.2	98.2
TS4 (C_1) + C_2H_2	40.7	150.0	144.5	133.4	140.7	137.5
TS5 (C_s,$^2A'$)	45.1	106.9	85.1	92.3	99.5	97.0
l-C_6H_4 (C_{2v}, $^1A_1$) + H	44.3	102.9	69.7	84.7	90.8	91.0

[a] ZPE calculated at B3LYP/6-31G(d) level. [b] The total energies (in hartree) for phenyl radical are the following: B3LYP/6-31G(d), −231.561 311 5; UMP2/6-311+G(3df,2p), −231.000 533; PUMP4/6-311G(d,p), −230.961 796; RCCSD(T)/6-31G(d), −230.855 839 3; G2M(rcc,MP2), −231.092 850 8.

system with six heavy atoms, we employ the G2M(rcc,MP2) approach, which improves the MP4/6-311G(d,p) base energy (E_{bas}) with the following corrections for basis set expansion and electron correlation:

$$\Delta E(\mathrm{RCC}) = E[\mathrm{RCCSD(T)/6\text{-}31G(d)}] - E[\mathrm{PMP4/6\text{-}31G(d)}]$$

$$\Delta E(+3\mathrm{df2p}) = E[\mathrm{MP2/6\text{-}311+G(3df,2p)}] - E[\mathrm{MP2/6\text{-}311G(d,p)}]$$

$$\Delta E(\mathrm{HLC,RCC6}) = -0.00493n_\beta - 0.00019n_\alpha$$

where n_α and n_β are the numbers of α and β valence electrons, respectively. The improved, ZPE-corrected energy with this scheme given in hartrees is

$$E[\mathrm{G2M(rcc,MP2)}] = E_{bas} + \Delta E(\mathrm{RCC}) + \Delta E(+3\mathrm{df2p}) + \Delta E(\mathrm{HLC,RCC6}) + \mathrm{ZPE}$$

The vibrational frequencies of all species involved in the reaction, including transition states (TSs), were calculated using the optimized geometries by the hybrid density functional B3LYP method (i.e., Becke's three-parameter nonlocal exchange functional[21]) and the nonlocal correlation functional of Lee, Yang, and Parr[22] with the 6-31G(d) basis set.[23] These frequencies were employed without scaling for ZPE corrections, characterization of stationary points, and transition-state theory (TST) as well as Rice−Ramsperger−Kassel−Marcus (RRKM) calculations.[24] All the energies cited below include ZPE corrections in units of kcal/mol. All the stationary points were identified by the number of imaginary frequencies (NIMF) with NIMF = 0 for a stable species and NIMF = 1 for a TS. Recently, the G2M(rcc,MP2) scheme has been applied to elucidate the kinetics and mechanism of the phenoxy radical decomposition reaction with reasonable success.[18]

All calculations were carried out with the Gaussian 92/DFT[25] and MOLPRO94[26] programs. The results of the calculations with these schemes are presented and discussed in the following section.

III. Results and Discussion

The computed geometries of various species are presented in Figure 1, and the energies obtained by different levels of theory and the vibrational frequencies and moments of inertia calculated at the B3LYP/6-31G(d) level are summarized in Tables 1 and 2, respectively. These results will be utilized for TST/RRKM calculations and discussion later.

A. The Decyclization Process. The decomposition of *c*-C_6H_5 by the ring-opening process represented by reaction a, as alluded to in the Introduction, has been widely assumed to be the sole unimolecular decay process.[11−16] Dewar and coworkers first investigated the decomposition process theoretically by the MINDO/3 method.[15] The energy barrier for ring opening was calculated to be 63.8 kcal/mol at 298 K. More recently, Walch reported the theoretical barrier, 72.0 kcal/mol, by the internally contracted configuration interaction (ICCI) method based on the geometry optimized by restricted Hartree−Fock (RHF) derivative calculations with the Dunning correlation consistent polarized valence double ζ basis set.[16] Our results, computed at various levels of theory based on the B3LYP/6-31G(d) optimized geometry for TS1, are presented in Table 1. The improved value, acquired by the G2M(rcc,MP2) scheme, 66.5 kcal/mol for the ring-opening process, agrees closely with the spin-projected UMP4/6-311G(d,p) and RCCSD(T)/6-31G(d) results, 65.6 and 69.4 kcal/mol, respectively. The three values lie between the earlier results of Dewar and Walch mentioned above.

The ring-opening process occurs at one of the two C−C bonds which increases from 1.404 to 2.48 Å at the transition state, TS1, with C_s symmetry. The product of the decyclization process, INT1 (1-dehydrohexa-1,3-dien-5-yne; HCĊH−cis) shown in Figure 1 also has C_s symmetry; it lies 60.9 kcal/mol above *c*-C_6H_5, suggesting that the barrier for recyclization is only 5.6 kcal/mol. That value compares reasonably well with 7.1 kcal/mol obtained by Walch with the ICCI method,[16] but is substantially lower than Dewar's value of 16.6 kcal/mol computed by MINDO/3.[15]

The INT1 intermediate isomerizes readily via TS2 to INT2 (1-dehydrohexa-1,3-dien-5-yne; HCĊH−trans) by bending the terminal C−H bond at the CH═ĊH radical site. The latter is less stable than the former by about 0.7 kcal/mol. The barrier for the isomerization reaction is calculated to be 4.0 kcal/mol, which may be compared with the value of 6.6 kcal/mol obtained by Walch, whose relative energies for INT1 and INT2 are 64.9 and 67.3 kcal/mol, respectively, above the *c*-C_6H_5 reactant.

B. The Decomposition of *l*-C_6H_5. Aside from the recyclization process, both *l*-C_6H_5 isomers can undergo fragmentation reactions producing *n*-C_4H_3 + C_2H_2 from INT2 via TS3 and *l*-C_6H_4 + H from either isomer via TS5. The structures of these TSs are presented in Figure 1. Schematically, the reactions can be given as follows:

$$l\text{-}C_6H_5 \xrightarrow{b} n\text{-}C_4H_3 + C_2H_2$$

$$\xrightarrow{d} l\text{-}C_6H_4 + H$$

Here, the two isomers are not distinguished because of the small energy difference and the convenience in performing multichannel RRKM calculations as discussed later.

TABLE 2: Molecular and Transition-State Parameters Used for RRKM Calculations

species or transition states	E_{rel}[a] (kcal/mol)	$I_aI_bI_c$ (amu)	ν (cm^{-1})		species or transition states	E_{rel}[a] (kcal/mol)	$I_aI_bI_c$ (amu)	ν (cm^{-1})	
phenyl radical	0.0	287.928	401.6	428.4	TS1	66.5	323.558	328.3i	233.2
		322.257	601.9	620.1			411.115	309.8	356.1
		610.185	671.8	721.8			734.674	457.5	482.0
			814.8	888.9				563.0	661.9
			954.6	985.6				699.3	754.9
			987.6	1024.3				759.3	881.3
			1060.7	1084.2				897.6	973.0
			1187.6	1189.0				1005.7	1053.7
			1319.3	1344.5				1221.3	1291.4
			1478.9	1492.0				1438.5	1565.6
			1595.6	1648.4				1643.9	2095.9
			3175.4	3181.8				3064.8	3180.7
			3195.4	3197.7				3201.0	3211.4
			3207.5					3478.1	
o-benzyne	24.4	257.438	396.1	411.7	TS3	105.6	364.066	277.1i	26.3[b]
		316.520	436.5	595.2			700.886	91.6	112.0
		573.958	621.9	754.1			1064.951	184.9	276.2
			843.3	870.3				354.8	575.2
			913.7	961.1				577.3	581.6
			1008.9	1087.4				585.2	634.1
			1117.1	1171.9				699.0	767.2
			1286.7	1339.9				769.9	855.2
			1439.4	1487.6				860.5	1052.1
			1502.5	2025.3				1285.4	1648.9
			3177.3	3193.2				1998.6	2218.6
			3215.7	3219.8				3054.7	3216.6
average of INT1 and INT2	61.3	277.565	109.9	141.4				3437.7	3494.8
		600.154	277.6	307.6				3522.3	
		877.719	465.1	501.0	TS5	96.5	277.084	688.7i	48.9
			575.4	623.7			688.337	117.1	243.2
			673.6	733.5			965.421	283.0	384.7
			770.6	862.7				474.1	505.2
			880.9	959.3				574.6	591.7
			981.6	1036.7				611.0	627.0
			1265.3	1300.9				629.3	750.4
			1447.1	1614.5				776.6	904.3
			1676.4	2204.4				968.4	1044.6
			3187.9	3278.4				1260.0	1431.7
			3494.4					1638.7	2112.6
								2218.6	3174.0
								3213.1	3483.5
								3494.9	

[a] Energies relative to the phenyl radical were calculated at the G2M(rcc,MP2) level, and the geometries and vibrational frequencies were obtained at the B3LYP/6-31G(d) level of theory. [b] Replaced with free internal rotation with $I_r = 17.38 \times 10^{-40}$ g·cm^2.

The barrier for the formation of *n*-C_4H_3 + C_2H_2 from INT2 was calculated to be 44.0 kcal/mol, which agrees closely with the value of Walch, 42.3 kcal/mol.[16] The barrier for the production of *l*-C_6H_4 + H was found to be 36.1 kcal/mol, which may be compared with the barrier for the *n*-C_4H_3 decomposition giving C_4H_2 + H via TS4, calculated at the same level of theory, 39.3 kcal/mol (see Table 1). These results clearly indicate that the production of *n*-C_4H_3 + C_2H_2 is less competitive than the formation of *l*-C_6H_4 + H at high temperatures when the *l*-C_6H_5 intermediates play a more significant role in the phenyl decomposition kinetics. The relative importance of these product channels will be compared with that of the recyclization process and the direct production of *o*-C_6H_4 + H from *c*-C_6H_5 below.

C. The Decomposition of *c*-C_6H_5 Producing *o*-C_6H_4 + H. The decomposition of the phenyl radical producing *o*-benzyne + H was found to be endothermic by 76.0 kcal/mol, and the reaction occurs without a distinct transition state; namely, the barrier for the reverse reaction was determined to be negligibly small. This might not be surprising because the reverse barrier for the analogous reaction d was calculated to be $E^\circ_{-d} = 6.0$ kcal/mol at the G2M(rcc,MP2) level of theory. Therefore, the addition of H to *o*-C_6H_4, which is almost 3 times more exothermic because of the restoration of the resonance structures, is expected to have a much smaller barrier.

In order to provide TS parameters for thermal rate constant calculations, to be described later, we have evaluated variationally along the reaction coordinate the total energies of the C_6H_4−H system for 14 different C−H separations at the B3LYP/6-31G(d) level of theory. The optimized relative energies and other molecular parameters are summarized in the table in Appendix A. The calculated electronic energies between r(C−H) = 2.3 Å and 2.9 Å (where the TS is located between 300 and 2500 K) are fitted to the Morse equation $E(r) = D'[1 - \exp(-\Delta r\beta)]^2$ by the least-squares method with $D' = 87.3$ kcal/mol and $\beta = 2.871$ Å^{-1} (average absolute deviation is less than 0.1%). For the canonical variational calculation of the decomposition of *c*-C_6H_5 with the TS located near the dissociation limit, *o*-C_6H_4, + H, the asymptotic region of the potential energy curve was rescaled with the G2M value to give $\Delta E(r) = D_{G2M}[1 - \exp(-\Delta r\beta)]^2 - D_{G2M}$, where $D_{G2M} = 76.0$ kcal/mol, as given in Table 1.

The dissociation energy as given, 76.0 kcal/mol, for the process *c*-$C_6H_5 \rightarrow$ *o*-C_6H_4 + H, agrees closely with the bond dissociation energy at 298 K, 77.5 ± 3.1 kcal/mol, recently reported by Davico et al.[27]

The PES of the C_6H_5 system, including all intermediates and product channels, is presented in Figure 2. The application of the PES for rate constant calculations, involving all coupled

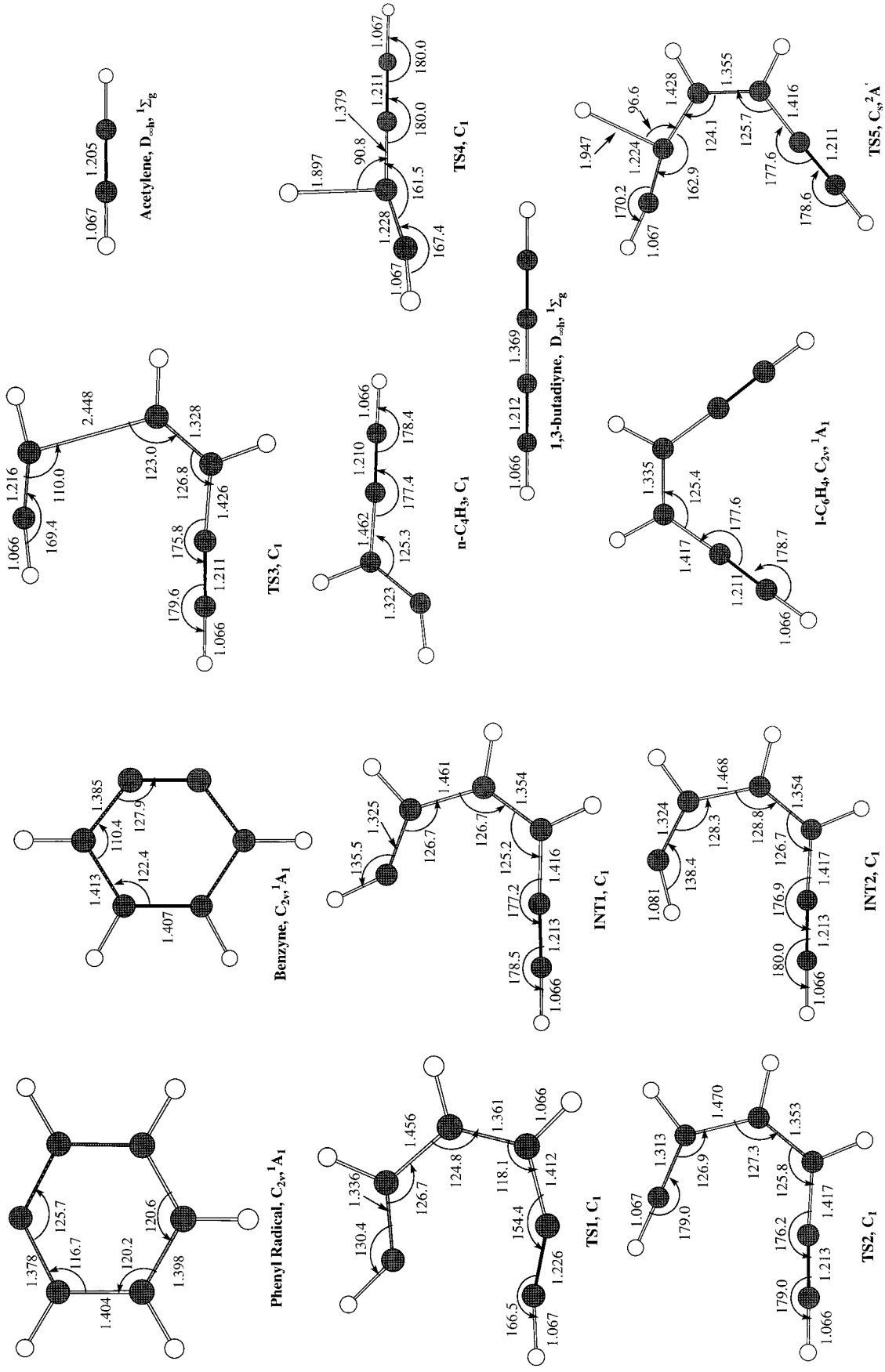

Figure 1. Geometries of various species involved in the decomposition of *c*-C_6H_5 calculated at the B3LYP/6-31G(d) level of theory.

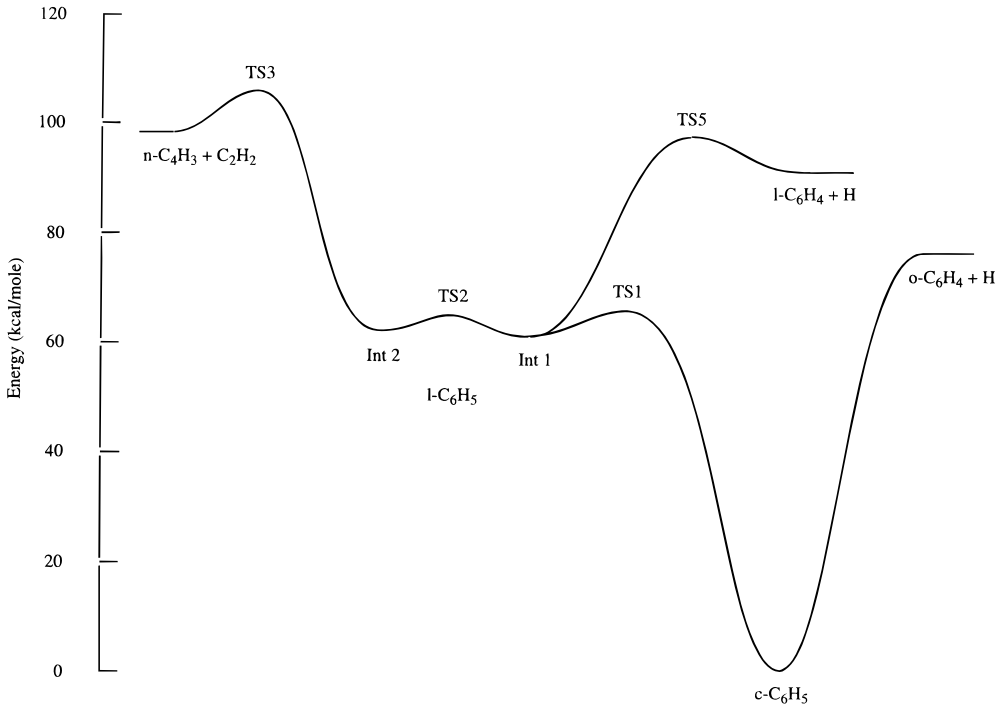

Figure 2. Potential energy surface of the C_6H_5 system at the G2M level of theory.

channels based on the RRKM theory, is discussed in the following section.

D. Thermal Rate Constant Calculations. *Unimolecular Decomposition of c-C6H5.* The rate constants for the formation of various products from *c*-C_6H_5 were computed with the following scheme:

$$c\text{-}C_6H_5 \underset{+M}{\overset{+M}{\rightleftharpoons}} c\text{-}C_6H_5^{\dagger} \underset{-a}{\overset{a}{\rightleftharpoons}} l\text{-}C_6H_5^{\dagger} \xrightarrow{b} n\text{-}C_4H_3 + C_2H_2$$

$$\xrightarrow{d} l\text{-}C_6H_4 + H$$

$$\xrightarrow{c} o\text{-}C_6H_4 + H$$

where "†" denotes internal excitation and M represents a third body.

For simplifying the RRKM calculations, we treated 1-dehydrohexa-1,3-dien-5-yne isomers, whose energies, moments of inertia, and vibrational frequencies are very close, as a single species, *l*-C_6H_5. We use their average energy, 61.3 kcal/mol above the reactant, in our calculations. The effect of this approximation on the calculated rate constants for reactions c, b, and d leading to key products of combustion interest is expected to be negligible.

The above reaction scheme is analogous to that employed for interpreting the NH_2 + NO product branching kinetics assuming H_2NNO and HNNOH as two key intermediates.[28] Accordingly, we employed the RRKM program which was previously written for the NH_2−NO system to model the decomposition kinetics of the C_6H_5 system with only minor modifications, i.e., the omission of collisional quenching for *l*-C_6H_5 because of its shallow well and the addition of the decomposition step for *c*-C_6H_5 via step c.

In our RRKM calculations, using the equations derived for the NH_2 + NO reaction by the steady-state method, tunneling corrections were not included. For tunneling corrections, the method developed by Diau and Lin[29] for the H + N_2O system may be applied. However, the RRKM program written for the reaction is applicable only to a reaction occurring by a single well or intermediate. For the present double intermediate case,

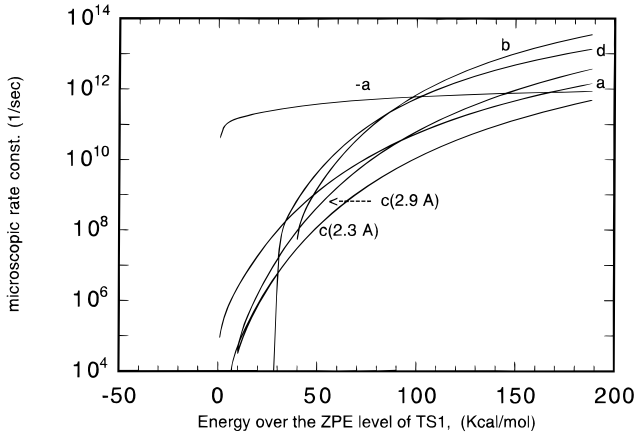

Figure 3. Specific rate constants for the decomposition of *c*-C_6H_5 and *l*-C_6H_5 as functions of the internal energy above TS1. (Tunneling correction included in the case of d.)

it is possible to use a new code prepared for calculations of the reaction system H + HNO ⇌ H_2NO ⇌ HNOH → HNO + H, in which the quantum-mechanical tunneling plays a significant role in the isomerization reaction.[30] For such a system, the direct solution of the coupled master equations calculating the production and decay of the chemically activated isomeric intermediates was carried out. The same approach could be adopted for the present system in which the fragmentation of *l*-C_6H_5 → *l*-C_6H_4 + H (d) exhibits a slight tunneling enhancement at low temperatures because of the existence of the reverse barrier, E°_{-d} = 6.0 kcal/mol, as indicated above. At temperatures of combustion interest, however, tunneling corrections are negligible and thus unnecessary.

The microcanonical unimolecular decay constants for reactions a, -a, b, c, and d are presented in Figure 3. Because reaction c lacks a well-defined TS, $k_c(E)$ is calculated with the transition-state parameters determined between two C−H separations, r(C−H) = 2.3 and 2.9 Å, corresponding to the locations with the maximum Gibbs free energies at 2500 and 300 K, respectively; the results for these two extreme cases are plotted in Figure 3. The procedure for evaluating $\Delta G^{\ddagger}$ with

TABLE 3: Unimolecular Rate Constants (in units of s^{-1}) for the Production of n-$C_4H_3 + C_2H_2$ (k_B), o-$C_6H_4 + H$ (k_C), and l-$C_6H_4 + H$ (k_D) from c-C_6H_5 as Functions of T and P[a]

	380 Torr			7600 Torr			1.0×10^{13} Torr		
T (K)	k_B	k_C	k_D	k_B	k_C	k_D	k_B	k_C	k_D
700	1.24×10^{-15}	1.59×10^{-9}	1.30×10^{-12}	1.26×10^{-15}	1.60×10^{-9}	1.31×10^{-12}	1.26×10^{-15}	1.60×10^{-9}	1.31×10^{-12}
1000	1.06×10^{-5}	2.80×10^{-2}	2.64×10^{-3}	1.15×10^{-5}	2.81×10^{-2}	2.72×10^{-3}	1.16×10^{-5}	2.81×10^{-2}	2.72×10^{-3}
1500	1.27×10^{2}	9.63×10^{3}	1.10×10^{4}	2.11×10^{2}	1.09×10^{4}	1.40×10^{4}	2.27×10^{2}	1.11×10^{4}	1.44×10^{4}
2000	8.51×10^{4}	2.46×10^{6}	4.68×10^{6}	3.11×10^{5}	5.06×10^{6}	1.05×10^{7}	4.85×10^{5}	6.53×10^{6}	1.34×10^{7}
2500	1.01×10^{6}	2.12×10^{7}	4.38×10^{7}	7.99×10^{6}	9.48×10^{7}	2.03×10^{8}	2.83×10^{7}	2.53×10^{8}	4.87×10^{8}

[a] Ar was assumed as the third-body with an average energy transfer step size of 300 cm^{-1} and collisional diameter of 5.27 Å. The atmospheric pressure data are given in the text by three-parameter Arrhenius equations.

the Morse potential $\Delta E(r)$ and the data given in Appendix A has been discussed elsewhere for such association processes as HCO + O_2[31] and $C_2H_3 + O_2$.[32]

The high-pressure, first-order rate constant calculated for reaction c with the equation

$$k_c = \frac{kT}{h} e^{-\Delta G_c^{\ddagger}/RT}$$

using the individually evaluated $\Delta G_c^{\ddagger}$ at T gives

$$k_c = 2.2 \times 10^{15} e^{-38{,}950/T}\ s^{-1}$$

The thermally averaged rate constants for the formation of the products of interest to combustion chemistry, n-$C_4H_3 + C_2H_2$, l-$C_6H_4 + H$, and o-$C_6H_4 + H$, directly from c-C_6H_5 at T and P, should be computed using the coupled reaction scheme to allow for the reversible ring-opening and -closing reactions as given by the full mechanism. The results of the calculations with the detailed equations (analogous to the ones employed for the $NH_2 + NO$ process as alluded to above) for 380, 7600, and 1.0×10^{13} Torr are summarized in Table 3. The results obtained for atmospheric pressure are plotted separately in Figure 4 for direct comparison with those for 1.0×10^{13} Torr pressure. A least-squares analysis of the atmospheric pressure data gives rise to the following expressions (in units of s^{-1}) for the unimolecular decomposition of c-C_6H_5 with the coupling of all open channels taken into consideration:

$$c\text{-}C_6H_5 \xrightarrow{B} n - C_4H_3 + C_2H_2,$$
$$k_B = 3.92 \times 10^{74} T^{-16.60} \exp(-68213/T)$$

$$c\text{-}C_6H_5 \xrightarrow{C} o\text{-}C_6H_4 + H,$$
$$k_C = 7.99 \times 10^{41} T^{-7.72} \exp(-46400/T)$$

$$c\text{-}C_6H_5 \xrightarrow{D} l\text{-}C_6H_4 + H,$$
$$k_D = 3.32 \times 10^{73} T^{-16.02} \exp(-64253/T)$$

for the temperature range 700−2500 K. As is evident from Figure 4, the rate constant for o-C_6H_4 production below 1500 K is greater than that for the formation of its linear isomer, l-C_6H_4, which is in turn is much larger than that for the fragmentation process, yielding the most commonly assumed products, n-$C_4H_3 + C_2H_2$. The former two processes producing the cyclic and linear C_6H_4 isomers become comparable above 1500 K because of the looser structures of l-C_6H_5 and TS5. Thus, the entropic factor overcomes the enthalpic deficit quickly for step d as the temperature of the system rises.

The effect of pressure at 1500 K for the decomposition of c-C_6H_5 via the three product channels is illustrated in Figure 5. The falloff rates of the first-order rate coefficients depend very strongly on the exit barriers due to the rapid depletion of the excited-state population by the decomposition via the lowest energy path, i.e., step c, which has the slowest falloff rate.

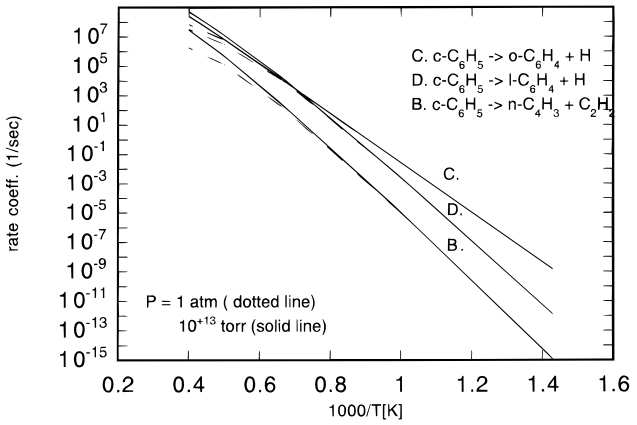

Figure 4. Temperature dependence of the first-order rate coefficients for production of o-$C_6H_4 + H$, l-$C_6H_4 + H$, and n-$C_4H_3 + C_2H_2$ from c-C_6H_5 at 1 atm and 1.0×10^{13} Torr pressure.

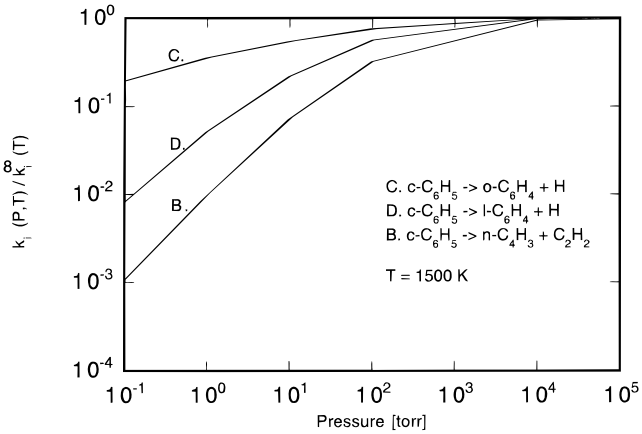

Figure 5. Pressure dependence of the first-order rate coefficients for the c-C_6H_5 decomposition reaction producing o-$C_6H_4 + H$, l-$C_6H_4 + H$, and n-$C_4H_3 + C_2H_2$ at 1500 K.

Bimolecular Reaction of n-C4H3 with C2H2. Both n-C_4H_3 and C_2H_2 may coexist in acetylene flames or in any hydrocarbon combustion system near sooting conditions. Therefore, we have also computed the overall rate constants for the production of l-C_6H_4, o-C_6H_4, and c-C_6H_5 from n-$C_4H_3 + C_2H_2$ by the rearranged reaction scheme involving the same elementary steps as before, viz.,

$$n\text{-}C_4H_3 + C_2H_2 \underset{b}{\overset{-b}{\rightleftharpoons}} l\text{-}C_6H_5^{\dagger} \xrightarrow{d} l\text{-}C_6H_4 + H$$
$$\underset{a}{\overset{-a}{\rightleftharpoons}} c\text{-}C_6H_5^{\dagger} \xrightarrow{c} o\text{-}C_6H_4 + H$$
$$\xrightarrow{+M} c\text{-}C_6H_5$$

RRKM calculations, using the same computer code with n-C_4H_3 and C_2H_2 as the reactants, give rise to the following rate

TABLE 4: Bimolecular Rate Constants (in units of cm^3 molecule^{-1} s^{-1}) for the Production of *o*-C_6H_4 + H ($k_{C'}$), *l*-C_6H_4 + H ($k_{D'}$), and *c*-C_6H_5 (k_M) from *n*-C_4H_3 + C_2H_2 as Functions of *T* and *P*[a]

	380 Torr			7600 Torr			1.0×10^{13} Torr		
T (K)	$k_{C'}$	$k_{D'}$	k_M	$k_{C'}$	$k_{D'}$	k_M	$k_{C'}$	$k_{D'}$	k_M
700	6.50×10^{-16}	1.34×10^{-13}	2.58×10^{-13}	3.37×10^{-17}	7.17×10^{-15}	2.61×10^{-13}	2.57×10^{-26}	5.47×10^{-24}	2.62×10^{-13}
1000	9.35×10^{-15}	5.44×10^{-12}	7.33×10^{-13}	6.02×10^{-16}	4.03×10^{-13}	7.95×10^{-13}	4.68×10^{-25}	3.18×10^{-22}	7.99×10^{-13}
1500	4.13×10^{-14}	7.10×10^{-11}	4.50×10^{-13}	7.13×10^{-15}	1.65×10^{-11}	7.47×10^{-13}	7.54×10^{-24}	1.97×10^{-20}	8.04×10^{-13}
2000	4.93×10^{-14}	1.30×10^{-10}	8.15×10^{-14}	2.29×10^{-14}	7.27×10^{-11}	2.97×10^{-13}	5.39×10^{-23}	1.98×10^{-19}	4.64×10^{-13}
2500	2.95×10^{-14}	9.77×10^{-11}	7.91×10^{-15}	2.27×10^{-14}	8.07×10^{-11}	6.22×10^{-14}	1.52×10^{-22}	6.17×10^{-19}	2.20×10^{-13}

[a] Ar was assumed as the third-body with an average energy transfer step size of 300 cm^{-1} and collisional diameter of 5.27 Å. The atmospheric pressure data are given in the text by three-parameter Arrhenius equations.

constants (in units of cm^3 molecule^{-1} s^{-1}) for 700−2500 K under the atmospheric pressure of Ar:

$$n\text{-}C_4H_3 + C_2H_2 \xrightarrow{D'} l\text{-}C_6H_4 + H,$$
$$k_{D'} = 2.25 \times 10^{13} T^{-6.10} \exp(-14838/T)$$

$$n\text{-}C_4H_3 + C_2H_2 \xrightarrow{C'} o\text{-}C_6H_4 + H,$$
$$k_{C'} = 7.16 \times 10^{8} T^{-5.97} \exp(-11910/T)$$

$$n\text{-}C_4H_3 + C_2H_2 \xrightarrow{M} c\text{-}C_6H_5,$$
$$k_M = 8.16 \times 10^{38} T^{-14.70} \exp(-15646/T)$$

For kinetic simulations under varying *T*,*P* conditions, we have presented in Table 4 the values calculated for three other pressures: 380, 7600, and 1×10^{13} Torr. Values for intermediate pressures and temperatures can be reasonably interpolated for practical applications.

IV. Concluding Remarks

In this work, we have investigated the unimolecular decomposition of the phenyl radical by combining ab initio MO and statistical theory calculations. The results of this study reveal for the first time that under thermal conditions C_6H_5 fragments to produce predominantly *o*-benzyne and a hydrogen atom by C−H breaking. The commonly assumed decyclization process, producing the 1-dehydrohexa-1,3-dien-5-yne radical (*l*-C_6H_5), which further fragments to yield *n*-C_4H_3 + C_2H_2, is the least significant channel of the three low-energy paths investigated. At very high temperatures ($T > 1500$ K), *l*-C_6H_5 decomposes more favorably to give *l*-C_6H_4 + H rather than *n*-C_4H_3 + C_2H_2. The formation of *l*-C_6H_4 (HC≡CCH=CH−C≡CH) under atmospheric pressure combustion conditions is predicted to be competitive with the production of its cyclic isomer, *o*-C_6H_4. Accordingly, for kinetic modeling of soot formation under practical conditions both *o*-C_6H_4 and *l*-C_6H_4 should be considered as the major decomposition products of the phenyl radical.

For practical modeling applications, we have calculated the thermal rate constants over a wide range of temperature and pressure with the RRKM theory employing the coupled multistep mechanism for the following six reactions:

$$c\text{-}C_6H_5 \rightarrow n\text{-}C_4H_3 + C_2H_2$$
$$c\text{-}C_6H_5 \rightarrow l\text{-}C_6H_4 + H$$
$$c\text{-}C_6H_5 \rightarrow o\text{-}C_6H_4 + H$$
$$n\text{-}C_4H_3 + C_2H_2 \rightarrow c\text{-}C_6H_5$$
$$n\text{-}C_4H_3 + C_2H_2 \rightarrow l\text{-}C_6H_4 + H$$
$$n\text{-}C_4H_3 + C_2H_2 \rightarrow o\text{-}C_6H_4 + H$$

Acknowledgment. The authors gratefully acknowledge the support received from the Department of Energy, Office of Basic Energy Sciences, Division of Chemical Sciences, through Contract DE-FGO5-91ER14191. We also thank the Cherry L. Emerson Center for Scientific Computation for the use of various programs and computing facilities.

Appendix A

Energies and Molecular Parameters of the C_6H_5 Structures Optimized at Various C−H Distances

R(C−H), Å	E_{rel},[a] kcal/mol	*i*	I_i, 10^{-40} g cm^2	υj (cm^{-1})
1.6	39.64	A	135.97	408, 436, 598, 618,659, 739, 843, 928,
		B	153.10	960, 977, 1025, 1052, 1054, 1080,
		C	288.99	1158, 1187, 1293, 1348, 1467, 1479,
				1580, 1647, 3181, 3196, 3203, 3216
1.7	49.57	A	135.97	407, 436, 594, 614, 654, 738, 841,
		B	153.54	923, 949, 972, 987, 1016, 1027, 1061,
		C	289.52	1140, 1186, 1281, 1346, 1464, 1470,
				1572, 1644, 3182, 3197, 3205, 3219
1.8	58.53	A	135.91	406, 436, 588, 609, 648, 736, 837,
		B	154.02	886, 934, 935, 944, 976, 1026, 1055,
		C	289.93	1132, 1185, 1275, 1345, 1461, 1467,
				1562, 1646, 3183, 3199, 3207, 3223
1.9	66.10	A	135.70	404, 437, 577, 604, 640, 728, 789,
		B	154.55	842, 848, 917, 929, 973, 1026, 1054,
		C	290.26	1128, 1183, 1273, 1343, 1457, 1472,
				1550, 1658, 3183, 3199, 3209, 3225
2.0	72.04	A	135.47	402, 435, 560, 601, 625, 668, 727,
		B	155.14	751, 849, 900, 926, 917, 1025, 1054,
		C	290.61	1126, 1182,1274, 1341, 1453, 1480,
				1538, 1676, 3183, 3199, 3210, 3225
2.1	76.47	A	135.25	399, 430, 540, 562, 597, 618, 632,
		B	155.28	748, 852, 885, 923, 969, 1023, 1055,
		C	291.07	1124, 1181, 1276, 1339, 1450, 1485,
				1528, 1699, 3183, 3199, 3212, 3225
2.2	79.65	A	135.13	388, 418, 493, 514, 520, 598, 622,
		B	156.58	748, 855, 874, 921, 968, 1020, 1056,
		C	291.70	1123, 1179, 1277, 1337, 1447, 1489,
				1519, 1722, 3182, 3198, 3214, 3225
2.3	81.91	A	135.11	350, 406, 424, 462, 498, 598, 615,
		B	157.34	759, 859, 865,920, 967, 1018, 1058,
		C	292.44	1123, 1177, 1279, 1334, 1445, 1491,
				1512, 1748, 3182, 3198, 3216, 3224
2.4	83.5	A	135.08	295, 349, 402, 453, 480, 598, 610,
		B	158.25	751, 859, 862, 919, 966, 1016, 1061,
		C	293.33	1122, 1176, 1280, 1333, 1444, 1493,
				1506, 1772, 3181, 3196, 3217, 3223
2.5	84.55	A	135.35	243, 285, 400, 448, 463, 599, 606,
		B	159.05	752, 854, 864, 918, 965, 1014, 1064,
		C	294.30	1121, 1175, 1282, 1331, 1443, 1495,
				1501, 1780, 3181, 3196, 3217, 3222
2.6	85.3	A	135.38	199, 233, 399, 445, 449, 601, 603,
		B	159.99	752, 851, 865, 916, 964, 1012, 1067,
		C	295.37	1120, 1174, 1283, 1330, 1441, 1496,
				1498, 1829, 3182, 3197, 3216, 3223
2.7	85.8	A	135.58	164, 191, 398, 441, 442, 600, 603,
		B	160.95	752, 848, 867, 916, 963, 1011, 1071,
		C	296.53	1119, 1174, 1284, 1330, 1441, 1494,
				1497, 1859, 3179, 3195, 3217, 3222
2.8	86.2	A	135.80	136, 156, 397, 429, 441, 600, 607,
		B	161.91	754, 847, 868, 915, 963, 1010, 1074,
		C	297.75	1119, 1174, 1284, 1330, 1441, 1493,
				1499, 1889, 3179, 3195, 3217, 3221
2.9	86.4	A	136.11	113, 128, 397, 422, 440, 598, 610,
		B	162.94	754, 846, 869, 915, 963, 1010, 1078,
		C	299.05	1118, 1174, 1285, 1329, 1441, 1491,
				1500, 1919, 3179, 3194, 3217, 3221

[a] Energy relative to phenyl radical, calculated at the B3LYP/6-31G(d) level. At infinite separation: $E_a = 87.3$ kcal/mol.

References and Notes

(1) Glassman, I. *Combustion*, 2nd ed.; Academic Press: 1987.

(2) Brezinsky, K. *Energy Combust. Sci.* **1986**, *12*, 1.

(3) McKinnon, J. T.; Howard, J. B. *24th Symp. (Int.) Combust., Proc.* **1992**, 965.

(4) Frenklach, M.; Clary, D. W.; Gardiner, W. C.; Stein, S. E. *20th Symp. (Int.) Combust. Proc.* **1985**, 887.

(5) Yu, T.; Lin, M. C.; Melius, C. F. *Int. J. Chem. Kinet.* **1994**, *26*, 1095.

(6) Frank, P.; Herzler, J.; Just, Th.; Wahl, C. *24th Symp. (Int.) Combust. Proc.* **1992**, 965.

(7) Yu, T.; Lin, M. C. *Combust. Flame* **1995**, *100*, 169.

(8) Yu, T.; Lin, M. C. *J. Am. Chem. Soc.* **1994**, *116*, 9571.

(9) Mebel, A. M.; Lin, M. C. *J. Am. Chem. Soc.* **1994**, *116*, 9577.

(10) Yu, T.; Lin, M. C. *J. Phys. Chem.* **1995**, *99*, 8599.

(11) Rao, V. S.; Skinner, G. B. *J. Phys. Chem.* **1984**, *88*, 5990.

(12) Rao, V. S.; Skinner, G. B. *J. Phys. Chem.* **1984**, *92*, 2442.

(13) Kiefer, J. H.; Mizerka, L. J.; Patel, M. R.; Wei, H.-C. *J. Phys. Chem.* **1985**, *89*, 2013.

(14) Braun-Unkoff, M.; Frank, P.; Just, Th. *22nd Symp. (Int.) Combust. Proc.* **1988**, 1053.

(15) Dewar, M. J. S.; Gardiner, W. C.; Frenklach, M.; Oref, I. *J. Am. Chem. Soc.* **1987**, *109*, 4456.

(16) Walch, S. P. *J. Chem. Phys.* **1995**, *103*, 8544.

(17) Mebel, A. M.; Morokuma, K.; Lin, M. C. *J. Chem. Phys.* **1995**, *103*, 7414.

(18) Liu, R.; Morokuma, K.; Mebel, A. M.; Lin, M. C. *J. Phys. Chem.* **1996**, *100*, 9314.

(19) Yokoyama, A.; Zhao, X.; Hintsa, E. J.; Continetti, R. E.; Lee, Y. T. *J. Chem. Phys.* **1990**, *92*, 4222.

(20) (a) Curtiss, L. A.; Raghavachari, K.; Trucks, G. W.; Pople, J. A. *J. Chem. Phys.* **1991**, *94*, 7221. (b) Pople, J. A.; Head-Gordon, M.; Fox, D. J.; Raghavachari, K.; Curtiss, L. A. *J. Chem. Phys.* **1989**, *90*, 5622. (c) Curtiss, L. A.; Jones, C.; Trucks, G. W.; Raghavachari, K.; Pople, J. A. *J. Chem. Phys.* **1990**, *93*, 2537.

(21) (a) Becke, A. D. *J. Chem. Phys.* **1993**, *98*, 5648. (b) *Ibid.* **1992**, *96*, 2155. (c) *Ibid.* **1992**, *97*, 9173.

(22) Lee, C.; Yang, W.; Parr, R. G. *Phys. Rev. B* **1988**, *37*, 785.

(23) Hehre, W.; Radom, L.; Schleyer, P. v. R.; Pople, J. A. *Ab Initio Molecular Orbital Theory*; Wiley: New York, 1986.

(24) Laidler, K. J. *Chemical Kinetics*, 3rd ed.; Harper and Row: New York, 1987.

(25) Frisch, M. J.; Trucks, G. W.; Head-Gordon, M.; Gill, P. M. W.; Wong, M. W.; Foresman, J. B.; Johnson, B. G.; Schlegel, H. B.; Robb, M. A.; Replogle, E. S.; Gomperts, R.; Andres, J. L.; Raghavachari, K.; Binkley, J. S .; Gonzales, C.; Martin, R. L.; Fox, D. J.; DeFrees, D. J.; Baker, J.; Stewart, J. J. P.; Pople, J. A. *GAUSSIAN 92/DFT*; Gaussian, Inc.: Pittsburgh, PA, 1993.

(26) Werner, H.-J.; Knowles, P. J. *MOLPRO94*; University of Sussex: Falmer, Brighton, 1994.

(27) Davico, G. E.; Bierbaum, V. M.; DePuy, C. H.; Ellison, G. B.; Squires, R. R. *J. Am. Chem. Soc.* **1995**, *117*, 2590.

(28) Diau, E. W. G.; Yu, T.; Wagner, M. G. A.; Lin, M. C. *J. Phys. Chem.* **1994**, *98*, 4034.

(29) Diau, E. W. G.; Lin, M. C. *J. Phys. Chem.* **1995**, *99*, 6589.

(30) Lin, M. C.; Hsu, C.-C.; Kristyan, S.; Melius, C. F. *Theoretical Study of the Isomerization and Decomposition of the H_2NO Radical*, Proc. 1996 JANNAF Combust. Meeting, in press.

(31) Hsu, C.-C.; Mebel, A. M.; Lin, M. C. *J. Chem. Phys.* **1996**, *105*, 2346.

(32) Mebel, A. M.; Diau, E. W. G.; Lin, M. C.; Morokuma, K. *J. Am. Chem. Soc.* **1996**, *118*, 9759.